06,16

Optical properties of $Sr_{0.6}Ba_{0.4}Nb_2O_6$ films on single-crystal MgO(001) and MgO(110) substrates

© Yu.V. Tekhtelev[1], N.V. Korchikova[1], A.V. Pavlenko[2,3]

[1] Lugansk State Pedagogical University,
Lugansk, Russia
[2] Scientific Research Institute of Physics, Southern Federal University,
Rostov-on-Don, Russia
[3] Southern Scientific Center, Russian Academy of Sciences,
Rostov-on-Don, Russia

E-mail: tehtelev@gmail.com

Received March 23, 2025
Revised April 7, 2025
Accepted April 7, 2025

The optical characteristics of $Sr_{0.6}Ba_{0.4}Nb_2O_6$ (SBN60) films of different thicknesses grown by RF cathodic sputtering in oxygen atmosphere on MgO(001) and MgO(110) substrates were studied using spectrophotometry and ellipsometry. It has been established that only when SBN60 films grow on MgO(110) substrates, a significant anisotropy of their optical properties is detected, which increases with decreasing film thickness. The reasons for the revealed regularities, as well as the role of the film nanostructure in the analysis of their optical properties, are discussed.

Keywords: thin films, magnesium oxide, barium-strontium niobate, spectrophotometry, ellipsometry.

DOI: 10.61011/PSS.2025.04.61271.56-25

1. Introduction

Segnetoelectric materials have been widely integrated in functional electronics, medical ultrasonic testing, defect inspection, microwave and piezo devices. The rapid development of micro- and nanoelectronics in recent decades has led to a great deal of attention in physical materials science to obtain and investigate the properties of nanoscale heterostructures based on segmentoelectric materials [1]. Uniaxial solid solutions $Sr_xBa_{1-x}Nb_2O_6$ are among one of the most promising film-scale segmentoelectric materials [2]. Segnetoelectric materials are also actively used in optoelectronics, fiber optics, and nonlinear optical devices due to their unique electro-optical and photorefractive properties. Optical parameters play a key role in device designing as they determine the interaction of light with the material, including phase modulation, wave propagation, and signal conversion efficiency. The anisotropy of optical properties is critical for creating polarization elements and waveguides, and precise values of film thickness and uniformity affect resonance characteristics and losses in multilayer structures. To measure these parameters, spectrophotometry (SPM) and ellipsometry (ELM) are complementary techniques. Spectrophotometry allows analyzing transmission spectra over a wide range of wavelengths, making it possible to estimate film thickness, detect optical gaps and structure defects. Ellipsometry, on the other hand, provides highly accurate determination of complex optical constants and film thickness. The combination of these techniques allows not only verification of the results, but also investigation of the influence of crystal orientation and surface morphology on the optical performance. In particular, this combined application of methods for $Sr_{0.6}Ba_{0.4}Nb_2O_6$ (SBN60) and $Sr_{0.5}Ba_{0.5}Nb_2O_6$ films on the MgO(110) substrate [3–5], helped to reveal anisotropy related to the orientation of the optical axis and to establish a correlation between structural features and functional properties, which is essential for process optimization and materials integration in next-generation devices.

The purpose of this paper is to study and analyze the optical properties of SBN60 thin films grown under the same conditions on MgO(001) and MgO(110) single crystal substrates.

2. Methods of sample preparation and study

Nanoscale barium-strontium niobate films with the composition $Sr_{0.6}Ba_{0.4}Nb_2O_6$ were synthesized by gas-discharge RF sputtering of the corresponding ceramic targets using complex oxide film deposition system „Plasma 50SE“ (manufactured by LLC „ELITECH“, Russia). A ceramic target of stoichiometric composition $Sr_{0.6}Ba_{0.4}Nb_2O_6$ with a diameter of 50 mm and a thickness of 3 mm was fabricated in the was fabricated at the Department of Materials Science and New Technologies, Research Institute of Physics, Southern Federal University (SFU). MgO(001) and MgO(110) single crystals of square shape with size 10×10 mm and thickness 0.5 mm were used as substrates,

the surfaces of which were prepared for heteroepitaxial deposition on both sides. The initial temperature of the substrate was ~ 673 K, increasing to 790–823 K during the film growth process after the discharge was applied, and the oxygen pressure in the chamber during the synthesis process was 0.5 Torr. The time of sputtering of the films on the MgO(001) substrate was 5, 15, and 100 min, and the time of sputtering of the films on the MgO(110) substrate was 25, 50, 100, and 120 min.

X-ray diffraction studies (phase composition, structural perfection of the films, lattice cell parameters, and orientation relationships between film and substrate) were performed using a multifunctional X-ray system „RIKOR“ ($Cu_{K\alpha}$-radiation).

The surface morphology of the studied films was studied using an atomic force microscope (AFM) „Ntegra Academia“ by NT-MDT. AFM topography scanning was performed in semi-contact mode using an NS15/50 silicon cantilever (probe radius of curvature ~ 8 nm, stiffness ~ 40 N/m, resonance frequency ~ 315 kHz) on areas of size 4 and 25 μm^2, scanning speed 0.9 Hz. The scanning quality was 400 dots per line for areas of 4 μm^2, and 512 dots per line for areas of 25 μm^2. The data were processed and visualized using Image Analysis software.

Optical transmission spectra were acquired using Shimadzu UV-2450 spectrophotometer at room temperature in the wavelength range of 200–900 nm. Ellipsometric measurements were performed using a multi-angle reflective null ellipsometer at the helium–neon laser wavelength (632.8 nm).

3. Experimental results and discussion

The study of SBN60/MgO(001) and SBN60/MgO(110) heterostructures by X-ray diffraction analysis found only bright reflections related either to the SBN60 film or to the MgO substrate. No traces of impurity phases were detected. Only reflexes of the (00l) family are detected in $\theta-2\theta$ X-ray diffraction pattern in normal scattering geometry for SBN60/MgO(001) heterostructures, indicating the orientation of the [001] axis along the normal to the substrate surface (the [001] axis of MgO). Only reflections of the ($hk0$) family are detected in the $\theta-2\theta$ X-ray diffraction pattern in normal scattering geometry for SBN60/MgO(110) heterostructures, indicating that the orientation of the polar axis [001] is parallel to the film-substrate interface plane. Considering that barium-strontium niobates are uniaxial materials in terms of optical properties, we used our results to interpret the experimental data presented below. Characteristic interference extrema (Figures 1, 2) are observed on the optical transmission spectra of the obtained heterostructures, the number of which increases with increasing film thickness.

The optical transmittance region of MgO substrates (curves *5*) is larger than that of the studied films. The numbers *2* and *3* in Figure 1 denote the transmission spectra

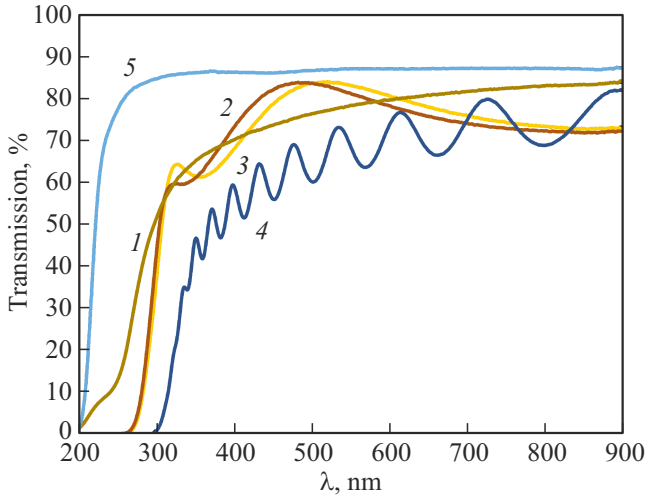

Figure 1. Transmission spectra of SBN60/MgO(110) films with different sputtering times: *1* — 5 min; *2* — 15 min (1); *3* — 15 min (2); *4* — 100 min; *5* — substrate MgO(001).

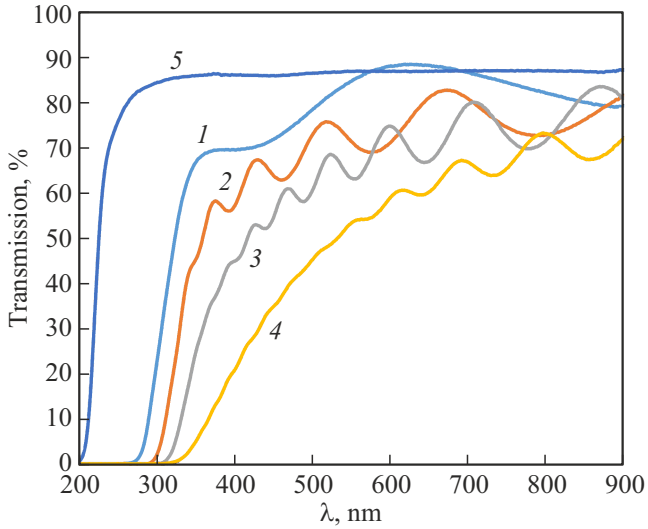

Figure 2. Transmission spectra of SBN60/MgO(110) films with different sputtering times: *1* — 25 min; *2* — 50 min; *3* — 100 min; *4* — 120 min; *5* — substrate MgO(110).

of the film with a sputtering time of 15 min taken at two different locations on the surface. Transmission spectra for SBN60/MgO(001) films were processed according to the procedure described in Ref. [6]. The calculation was not performed on film 5 min (*1*) because one extremum is not enough. The calculated thicknesses are provided in Table 1. We also calculated the refractive index dispersion for the film with sputtering time 120 min (Figure 3): the values well „fit“ into the dispersion curve n_o for the SBN61 crystal, and hence the optical axis of the film is perpendicular to the substrate.

The exact thicknesses of the SBN60/MgO(001) films and their surface character were determined by the ellipsometric

Table 1. Results of optical studies of the films SBN60/MgO(001)

t, min	d, nm			n ($\lambda = 632$ nm)	n_{ef} ($\lambda = 632$ nm)
	SPM	ELM			
		Main layer	Disturbed layer	ELM	
5	–	30	3	2.314	1.74
15 (1)	103	111	6	2.374	2.23
15 (2)	93	107	20	2.342	1.77
100	795	755	28	2.334	2.11

method [7]. Measurements were made for an isotropic bilayer film model, which includes a base transparent layer with thickness d and refractive index n and a disturbed layer with effective parameters d_{ef} and n_{ef}. The results of ellipsometric measurements are summarized in Table 1. The film-substrate boundary layer was not detected.

Figure 4 shows plots of the dependence of the ellipsometric angles Ψ and Δ on the angle of incidence φ for one of the films with sputtering time 100 min.

It can be noted (Table 1) that the thicknesses of SBN60/MgO(001) films determined by the two optical methods are in good agreement with each other. This indirectly indicates the homogeneity of the film during its growth.

Under normal incidence of partially polarized light, shifts in the transmission spectra of SBN60/MgO(110) films were detected at different film rotation angles around the axis Z perpendicular to the substrate surface. This often indicates that the optical axis of the film is at an angle to the Z axis. We analyzed the interference extrema

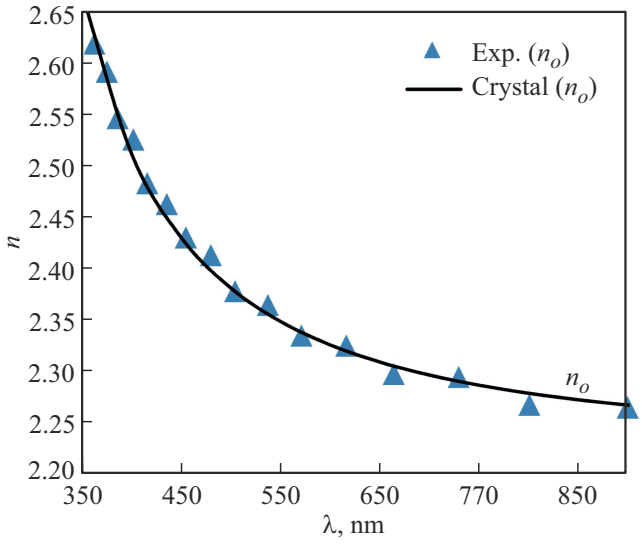

Figure 3. Dispersion of the refractive index of the film SBN60/MgO(001) ($t = 100$ min).

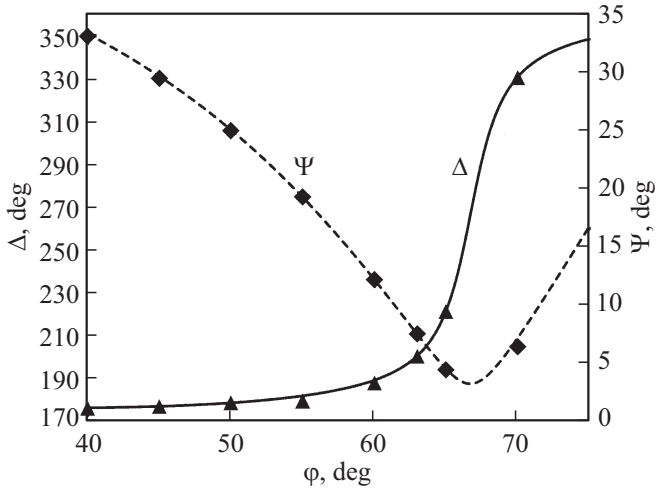

Figure 4. Calculated dependencies $\Psi(\varphi)$ and $\Delta(\varphi)$ for the film SBN-60/MgO(001) ($t = 100$ min).

and their intensities on the optical transmission spectra for determining the ordinary n_o and extraordinary n_e refractive indices and their dispersion in the transparency region of the SBN60/MgO(110) film with thickness $d > \lambda/2$. Generally, the direction of the optical axis on the film surface is unknown, but can be established by taking spectra in different planes of incidence. Thus, in an isotropic plane of incidence perpendicular to the optical axis, the intensity of the transmitted light is maximal, and in a plane of incidence parallel to the optical axis — minimal. In addition, the corresponding interference extrema are maximally shifted in wavelengths in these planes, since the phase thickness of the film in these planes is equal to

$$n_o d = m\frac{\lambda^{(o)}}{2} \quad \text{and} \quad n_e d = m\frac{\lambda^{(e)}}{2}, \tag{1}$$

where m is the order of the interference extremum $\lambda^{(0)} > \lambda^{(e)}$.

The ratio $n^{(0)}/n^{(e)} = \lambda^{(0)}/\lambda^{(e)}$ can be found by measuring the wavelengths $\lambda^{(0)}$ and $\lambda^{(e)}$ at fixed m on the spectra obtained in the planes of normal incidence of a plane

Table 2. Results of optical studies of the films SBN-60/MgO(110)

t, min	d, nm			Δn (SPM)	n (ELM)
	SPM	ELM			
		Main layer	Disturbed layer		
25	135	122 131	64 54	–	$n_o = 2.318$ $n_e = 2.282$
50	442	424 426	41 28	$\Delta n \approx 0.020$	$n_o = 2.314$ $n_e = 2.290$
100	775	736 745	38 29	$\Delta n \approx 0.013$	$n_o = 2.318$ $n_e = 2.302$
120	1048	1010 1012	41 36	$\Delta n \approx 0.008$	$n_o = 2.314$ $n_e = 2.310$

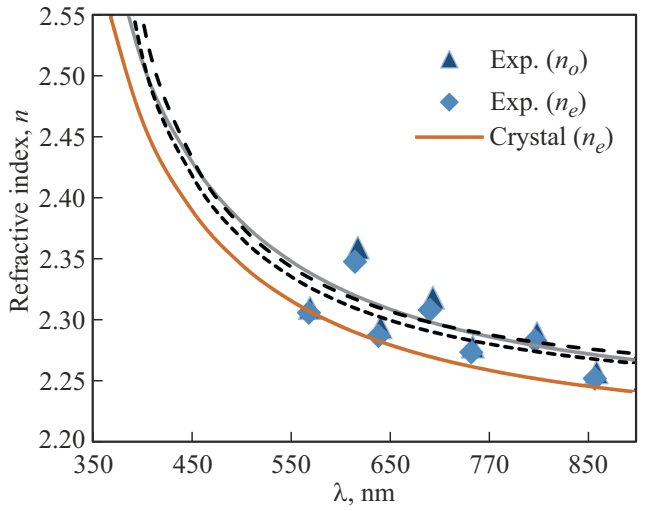

Figure 5. Dispersion of the refractive indices of the film SBN-60/MgO(110) ($t = 120$ min).

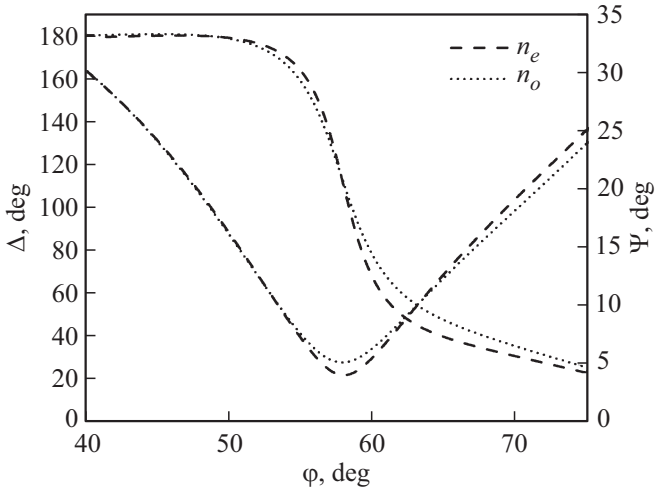

Figure 6. Calculated dependences $\Psi(\varphi)$ and $\Delta(\varphi)$ for SBN60/MgO(110) film ($t = 120$ min).

electromagnetic wave parallel and perpendicular to the direction of the optical axis. Thus, we can find the dependences of n_o and n_e on the wavelength by determining the film thickness in an independent way.

This calculation was performed for all the films studied except 25 min, because there is only one clear extremum on the transmission spectrum (Table 2). Zellmeyer formula was used for interpolating the theoretical values.

Figure 5 shows the dispersion of n_o and n_e for one of the SBN-60/MgO(110) films with sputtering time of 120 min.

Analysis of variance n_o and n_e showed that the difference of values $\Delta n = n_o - n_e$ decreases with the increase of film thickness in the considered series of samples. However, the value is $\Delta n \geq 0.026$ for crystals of similar composition [8]. This change Δn indicates that the dimensional effects manifested in nanoscale structures play a significant role in shaping the optical characteristics, and in our case this is most clearly seen for n_e. This may be attributable to the fact that the temperature blurring of the phase transition region from the paraelectric to the segmentoelectric phase in SBN films increases when compared with single crystals [2]. According to Ref. [9] significant changes in optical characteristics occur in SBN crystals, regardless of the composition, specifically in the vicinity of PE → SE, in particular the sign of optical anisotropy changes first as the temperature decreases, and then the value of n_o practically does not change, and n_e monotonically decreases. It is reasonable to assume that this is the effect we are capturing.

The exact values of the thickness of the films and the nature of their surface were determined by the ellipsometric method [7]. Measurements were made along the directions corresponding to the directions of MgO [001] and [−110] for an isotropic two-layer film model, which includes a base transparent layer of thickness d with refractive index n and a disturbed layer with effective parameters d_{ef} and n_{ef}. The results of ellipsometric measurements are summarized

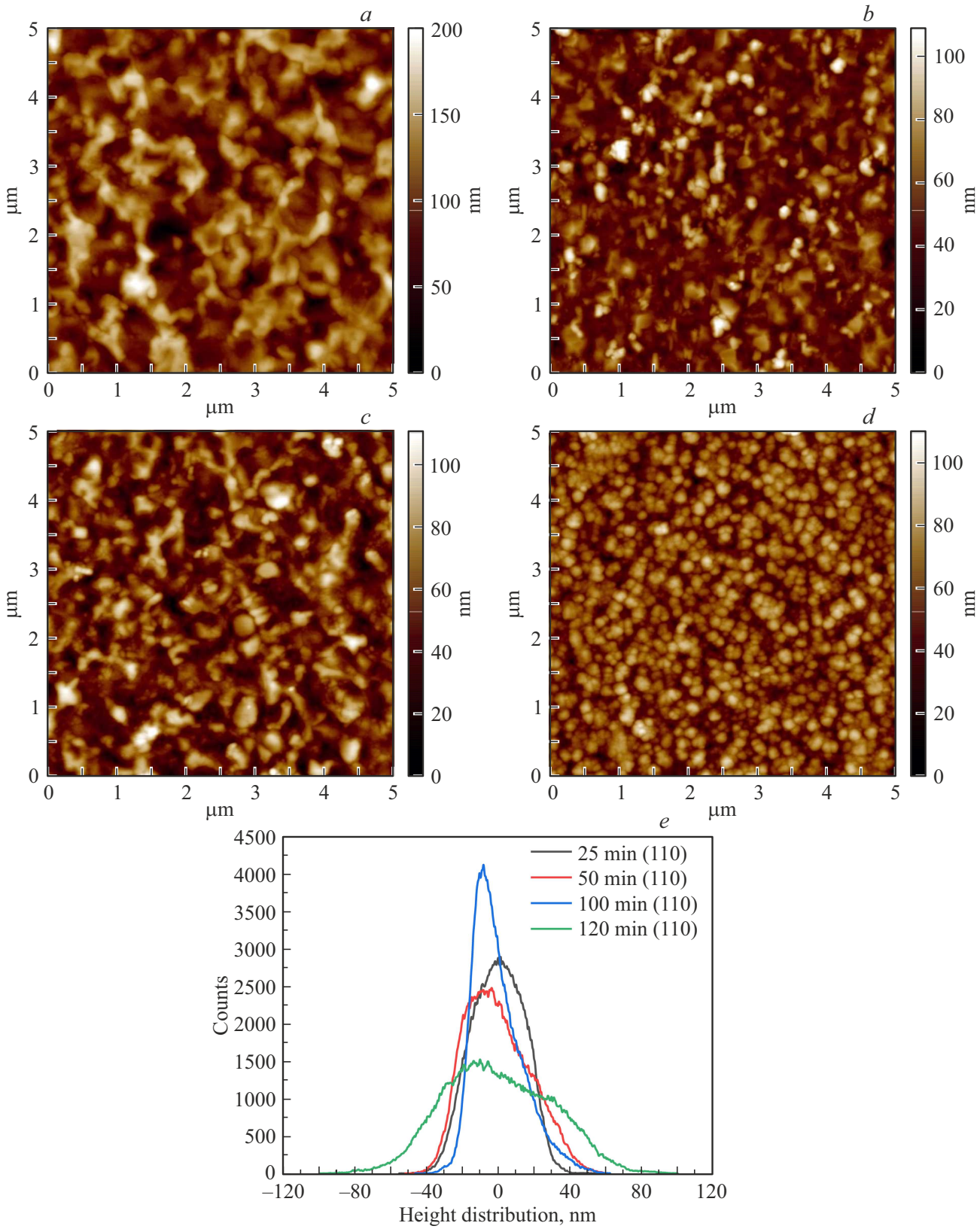

Figure 7. AFM images of the surface topography of SBN60/MgO(110) heterostructures with different sputtering times (*a* — 25 min, *b* — 50 min, *c* — 100 min, *d* — 120 min). *e* — histogram of height distribution for surface areas *a*–*d*.

in Table 2. The boundary layer film–substrate was not detected.

Figure 6 shows plots of the dependence of ellipsometric angles on the angle of incidence for one of the films with sputtering time 120 min.

Table 2 shows that for films with sputtering times of 100 and 120 min, the thicknesses found by the two optical methods agree well. The thicknesses of films with sputtering times of 25 and 50 min no longer agree. This is attributable to the fact that the spectra calculation methodology does not take into account the significant contribution of the surface layer, but considers the whole film as a single unit.

It can be seen from the transmission spectra (Figure 2) that extrema are „blurred" with the increase of the film thickness SBN-60/MgO(110) and they become almost invisible at wavelengths of 350–500 nm on the thickest film, as they are close enough to each other. This effect is also present on thinner films, but less, commensurate with their thickness. „Smoothing" of the extrema causes them to shift in wavelength, causing the points to be located above and below the theoretical dispersion curve (Figure 2). This behavior cannot be attributed to light scattering in the surface layer, because its value varies weakly on all films. This effect is not observed for the films on MgO(001) substrate (Figure 1), and its cause may be the peculiarities of growth of barium-strontium niobate films on MgO(110) substrates.

Figure 7 summarizes the results of the studies of the surface nanostructure of SBN60/MgO(110) films.

It is well seen that the structure of its surface gradually changes as the thickness of the SBN60 film increases — the enlargement of growth blocks occurs, and both their lateral size and vertical size increase significantly. This can be clearly seen from the histogram of height distribution on the surface of the films presented in Figure 7, *e*. The minimum RMS surface roughness of 14.3 nm was observed in the case of the thinnest SBN60 film, and as its thickness increased, it gradually increased and reached 29.8 nm for the SBN60 film with sputtering time 120 min. This evolution of the nanostructure indicates that the obtained SBN60 films under the used technological conditions grow according to the Wolmer–Weber mechanism (island growth mechanism). To date, we have not been able to unequivocally determine whether the SBN60 films we obtained on MgO(110) substrates are single-crystalline or highly textured. The patterns of nanostructure formation of films depending on their thickness that we have identified can be manifested in both single-crystalline films and polycrystalline films [10]. As the analysis of the literature has shown, unfortunately, at present there is no information on a similar type of studies for barium-strontium niobates or closely related segmentoelectrics with a TTB-type structure. However, we believe that by varying the modes of film preparation it will be possible to achieve both improvement of the surface quality of the films and their structural perfection. We plan to realize this in future studies.

4. Conclusion

1. A series of undoped heterostructures SBN60/MgO(001) and SBN-60/MgO(110) with different thicknesses of SBN60 films were obtained using the high-frequency cathodic sputtering method in oxygen atmosphere, wherein the [001] axis of the film in SBN60/MgO(001) was oriented along the normal to the substrate surface, and it was oriented parallel to the film-substrate interface plane in SBN60/MgO(110).

2. The thicknesses of SBN60 films on single crystal MgO substrates and the dispersion of refractive indices have been determined by spectrometric and ellipsometric methods. It is shown that a significant anisotropy of optical properties is found only on MgO(110) substrates under identical modes of sputtering of SBN60 films.

3. Calculation of dispersion dependences based on the transmission spectra showed that the refractive index difference Δn decreases with the increase of SBN60/MgO(110) film thickness, which may indicate structural changes in the studied films. This is indirectly indicated by „smoothing" of the transmission spectra.

Funding

The study was financially supported by the Ministry of Science and Higher Education of the Russian Federation (Project No. FENW-2023-0010/GZ0110/23-11-IF).

Acknowledgments

Equipment provided by the „Joint Scientific and Technological Equipment Center of the Southern Scientific Center of the Russian Academy of Sciences (Research, Development, Testing)" shared research facility was used in the study.

Conflict of interest

The authors declare no conflict of interest.

References

[1] K.A. Vorotilov, V.M. Mukhortov, A.S. Sigov. Integrirovannye segnetoelektricheskie ustroystva. Energoatomizdat, M. (2011). 175 p. (in Russian).

[2] A.V. Pavlenko, S.P. Zinchenko, D.V. Stryukov, A.P. Kovtun. Nanorazmernye plenki niobata bariya-strontsiya: osobennosti polucheniya v plazme vysokochasotnogo razryada, struktura i fizicheskie svoistva. Izdatelstvo YuNTs RAN, Rostov-na-Donu. (2022). 244 p. (in Russian).

[3] S.V. Kara-Murza, N.V. Korchikova, A.G. Silcheva, Yu.V. Tekhtelev, R.G. Chizhov, K.M. Zhidel, A.V. Pavlenko. PHENMA 2021–2022: Abstracts and Schedule. Southern Federal University Press, Rostov-on-Don. 147 (2022).

[4] Y.V. Tekhtelev, R.G. Chizhov, K.M. Zhidel, S.V. Kara-Murza, A.V. Pavlenko, A.G. Silcheva. LFPM–2021 **2**, *10*, 133 (2021). (in Russian).

[5] Y.V. Tekhtelev, N.V. Korchikova, A.G. Silcheva, A.V. Pavlenko. LFPM–2024 **2**, *13*, 246 (2024). (in Russian).
[6] S.V. Kara-Murza, N.V. Korchikova, Y.V. Tekhtelev, K.M. Zhidel, A.V. Pavlenko, L.I. Kiseleva. Journal of Advanced Dielectrics **11**, *5*, 2160014 (2021).
[7] A.A. Tikhiy, V.A. Gritskikh, S.V. Kara-Murza, N.V. Korchikova, Y.M. Nikolaenko, V.V. Faraponov, I.V. Zhikharev. Optika i spektroskopiya **119**, *2*, 282 (2015). (in Russian).
[8] D. Kip, S. Aulkemeyer, K. Buse, F. Mersch, R. Pankrath, E. Krätzig. Physic Status Solidy (a) *151*, K3 (1996).
[9] Yu.S. Kuzminov. Segnetoelektricheskie kristally dlya upravleniya lazernym izlucheniem. Nauka, M. (1982). p. 400. (in Russian).
[10] S.A. Kukushkin, A.V. Osipov. UFN, **168**, *10*, 1083 (1998). (in Russian).

Translated by A.Akhtyamov